Materials Today • Volume xxx, Number xx • xxxx 2023 RESEARCH

ELSEVIER

Strongly enhanced charge density via gradient nano-doping for high performance elastic-material-based triboelectric nanogenerators

Xiaobo Gao [1,4,†], Fangjing Xing [2,3,†], Feng Guo [1,*], Jing Wen [2,3], Hao Li [2,3], Yuhan Yang [2,3], Baodong Chen [2,3,4,*], Zhong Lin Wang [2,3,5,*]

[1] School of Materials Science and Engineering, Inner Mongolia University of Technology, Hohhot 010051, PR China
[2] Beijing Institute of Nanoenergy and Nanosystems, Chinese Academy of Sciences, Beijing 101400, PR China
[3] School of Nanoscience and Technology, University of Chinese Academy of Sciences, Beijing 100049, PR China
[4] Institute of Applied Nanotechnology, Jiaxing, Zhejiang 314031, PR China
[5] Georgia Institute of Technology, Atlanta, GA 30332, USA

Elastic-material-based triboelectric nanogenerators (EMB-TENGs) are most effective to harvest random (low frequency, low amplitude) and distributed mechanical energy. However, the low output of EMB-TENGs caused by drastic charge attenuation and low sensitivity limits its applications. Here, we propose a gradient nano-doping strategy to boost the charge density and sensitivity of triboelectric sponge materials via the gradient electrical field caused by the inhomogeneous concentration field of polytetrafluoroethylene nanoparticles. The triboelectric charge density (537 $\mu C \cdot m^{-3}$) and the peak power density (732.6 $mW \cdot m^{-3}$) is increased by 1.2 times and 1.8 times. A sensitivity of 1.851 kPa^{-1} is successfully realized at 50% compressive strain. From this, a self-powered smart boxing bag with functions of both the force analysis and real-time counting statistic was developed at the large strain. This work presents a new method for design and development of triboelectric materials, as well as expanding the functionalities and applications of self-powered system combining with the EMB-TENGs.

Keywords: Triboelectric nanogenerator; Gradient nano-doping; Triboelectric sponge; Charge density; Self-powered system

Introduction

With the developing of 5G and the Internet of Things (IoTs), more and more acquisition and utilization clean energy are attracted a growing number of researchers' attention [1–3]. Because such devices and sensors consume electrical power continuously, the acquisition of distributed energy has increased. However, traditional fossil fuels are not only polluting the environment, but are also non-renewable and unaccommodated [4,5]. Traditional power supply methods such as the cable transmission and the battery power supply are costly and have difficulties in supplying power to sensors that are widely distributed and remotely located [6–13]. Researchers have looked variously for supplying power and energy harvesters, such as thermoelectric nanogenerators (TEGs) [14–16], piezoelectric nanogenerators (PENGs) [17,18] and electromagnetic generators (EMGs) [19,20], which can harvest various types of energy, including wind energy [6,21–26], ocean energy [27–33], vibrational energy [34,35] and motion energy [36]. In 2012, the triboelectric nanogenerators (TENGs, also called as Wang generator) [37–40], based on the coupling effect of contact electrification and electrostatic induction was invented that is not only a

* Corresponding authors.
E-mail addresses: Guo, F. (guofengnmg@sina.com), Chen, B. (chenbaodong@binn.cas.cn), Wang, Z.L. (zlwang@gatech.edu).
† X. G., and F. X., these authors contributed equally to this work.

 https://doi.org/10.1016/j.mattod.2023.03.010

Please cite this article in press as: X. Gao et al., Materials Today (2023), https://doi.org/10.1016/j.mattod.2023.03.010

promising technology for converting mechanical energy into electricity, owing to its advantages of lightweight, high efficiency, small size and a wide choice of materials, but it is also used as active sensors, because TENG has good adaptability to various forms of mechanical motion, and the output signal of TENGs can well reflect the change of mechanical excitation, so it is considered to be the potential solution of self-powered sensing [41–46].

Meanwhile, tremendous efforts have been devoted to improve the elastic-material-based triboelectric nanogenerators (EMB-TENGs) by a series of elastic triboelectric materials, such as polyurethane sponge (PU), ethylene–vinyl acetate copolymer (EVA), and porous silicone rubber elastomer. The micro-porous foams have been used to develop EMB-TENGs to replace other synthetic polymers, but the low elasticity of such foams makes devices less adaptable. The elastic polyurethane sponges have the advantages of low density, high porous network structure, moderate mechanical properties, high specific surface area for exploring EMB-TENGs is an ideal triboelectric material system. The EMB - TENG is a promising energy technology to drive billions of micro-electronics in the outdoor environments in a self-powered manner. To boost the output performance, various methods of material modification [47], structural optimization, surface patterning treatment [48], charge pump and environment control [49,50] are proposed. In addition, even though extensive progress has been achieved in the exploration of compressible EMB-TENGs and super-elastic triboelectric materials, the output performance and sensing sensitivity of strain-induced triboelectric materials remain to be improved. And the low output of EMB-TENGs caused by drastic charge attenuation and low sensitivity limits its applications [51–56].

In this work, we propose a gradient nano-doping strategy to boost the charge density and sensing sensitivity of EMB-TENG by incorporating polytetrafluoroethylene (PTFE) nanoparticles in polyurethane sponge via gradient electrical field caused by the inhomogeneous concentration field of PTFE. Gradient nano doped refers to the doping of dielectric materials with different concentrations in the upper and lower layers of polyurethane materials. We first investigate the interaction electrodynamics of the gradient electrical field and the inhomogeneous concentration to obtain the optimal boundaries of gradient nano-doping. The electrical behaviors can be described as the directional accumulation of electric charges under gradient electrical field. The triboelectric charge density (537 $\mu C \cdot m^{-3}$) and the peak power density (732.6 $mW \cdot m^{-3}$) is increased by 1.2 times and 1.8 times at the gradient ratio of 3:1, respectively. The sensitivity of 1.851 kPa^{-1} which in 50% strain compressive status is successfully realized. In addition, the sensitivity of the electrical signal is extremely high (about 1.851 kPa^{-1}) which in 50% strain compressive status compared with the previously suggested energy-harvesting devices, which ensures the overwhelming electrical output-performance of the current EMB-TENG. Furthermore, the EMB-TENG can be applied to a smart boxing bag to achieve punches data statistics and strike force sensing, and a self-powered pugilism training system is successfully demonstrated. This work proposes a novel strategy for designing and optimizing of triboelectric materials, demonstrate that EMB-TENGs can be easily developed for the large-scale energy harvesting and pressure sensing at the large strain, with simple preparation process, controlled quality, low cost, and weight.

Results and discussion

Nano-doping elastic triboelectric sponge is prepared via a simple room temperature foaming method by incorporating PTFE nano-powder on the surface of the polyurethane sponge's three-dimensional skeletal matrix structure. The preparation process of the nanocomposite triboelectric sponge is shown in Fig. 1**a**, and the molecular formulas of polyurethane and PTFE are shown in Fig. 1**b**, the detailed preparation foaming process is shown in Experimental Section and Supporting Information **Fig. S1**. The appearance of the prepared triboelectric sponge has a porous structure as shown in Fig. 1**c**. In order to characterize the morphology of the porous structure of the prepared triboelectric sponge and its physical properties with foaming ratio of 2:1, such as pore size, porosity, and permeability, three-dimensional profile scanning and mercury intrusion tests were performed, and the results are shown in Fig. 1**d and e**. The morphology of the prepared sponge with foaming ratio of 3:1 is shown in **Fig. S2**. In the mercury intrusion test, the polyurethane with a mass of 0.02 g was selected for testing, the total pore volume was 1.12 mL/g, the total pore area was 0.085 m^2/g, the average pore diameter was 52.83 μm, the porosity was 48.35%, and the permeability was 34665.64 md. Therefore, the foamed polyurethane has higher elastic properties. A shore durometer was used to test the hardness of foamed polyurethane, and the results are shown in Fig. 1**f**. The results show that Shore Hardness (SH) decreases with the increase of the foaming ratio of polyether polyol and isocyanate, and increases with the doping content of PTFE nano-power, but the increase is not obvious. Due to the small SH value, the practical application of foamed polyurethane is limited, so all subsequent experiments and applications choose the highest SH value (foaming ratio was 2:1). Material modification is one of the main methods commonly used to improve the performances. In order to improve the charge density and triboelectric sensitivity of the elastic polyurethane triboelectric sponge, we selected PTFE nano-powder with high dielectric constant as the doped nanocomposite to make it adhere to the surface of the polyurethane sponge's three-dimensional skeletal matrix structure. Fig. 1**g**-i show scanning electron microscope (SEM) photos of the mass percentage of doped PTFE being 0%, 1%, and 3%, respectively. With the increase of doping content, more PTFE is attached on the surface of polyurethane, which provides reliable data support for the following experiments. The detailed SEM photos are shown in **Fig. S3** of Supporting Information.

Working mechanism of EMB-TENG is shown in Fig. 2, which illustrates the coupling effect of triboelectrification and electrostatic induction. Based on the fabricated polyurethane triboelectric sponge as functional dielectric layer, and due to the conductivity of copper (Cu) film which it can work as both triboelectric layer and electrode. Therefore, the working mode of EMB-TENG based on fabricated triboelectric sponge is a single electrode mode, and its working principle is shown in Fig. 2**a**. In the initial state, the polyurethane triboelectric sponge doped with PTFE contacts with the Cu film, negative triboelectric

Please cite this article in press as: X. Gao et al., Materials Today (2023), https://doi.org/10.1016/j.mattod.2023.03.010

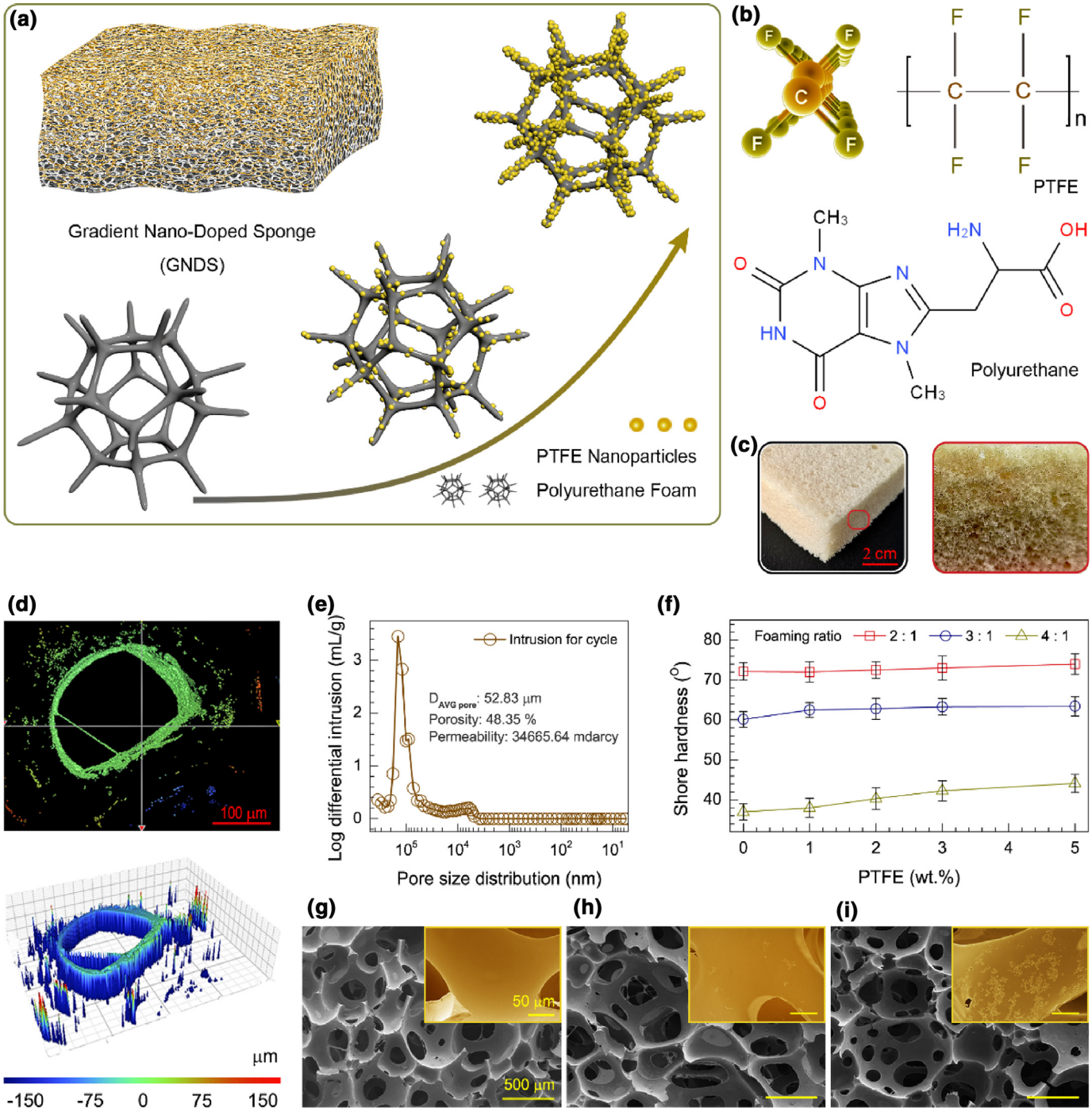

FIGURE 1

Schematic diagram of the structure, properties, and morphology of the gradient nano-doped triboelectric materials. (a). Schematic illustration showing the structure design of the gradient nano-doped triboelectric materials. Gradient nano doped refers to the doping of dielectric materials with different concentrations in the upper and lower layers of polyurethane materials. (b). Schematic diagram of the doped PTFE nanoparticles and polyurethane. (c). The photograph of the gradient nano-doped triboelectric materials. (d). Three-dimensional contour of pore structure with the foam ratio of 2:1. (e). The porosity of the triboelectric materials. (f) Hardness of the triboelectric materials with the different foaming ratios and PTFE doping amounts. SEM images of the bottom surfaces of the triboelectric materials with the different PTFE content (wt. %): (g) Nano-doping PTFE of 0%, (h) Nano-doping PTFE of 1%, (i) Nano-doping PTFE of 3%.

charges are gained by the polyurethane due to its stronger ability to capture negative charges, whereas the surface of Cu electrode is left positive charged (i). When the force begins to press with the triboelectric sponge, the potential difference between the two surfaces will gradually increase, leading to an instantaneous electron flow from the ground to the Cu electrode in the external circuit (ii). This transient flow of the electrons continues until the triboelectric sponge was totally pressed (iii). When the force

Please cite this article in press as: X. Gao et al., Materials Today (2023), https://doi.org/10.1016/j.mattod.2023.03.010

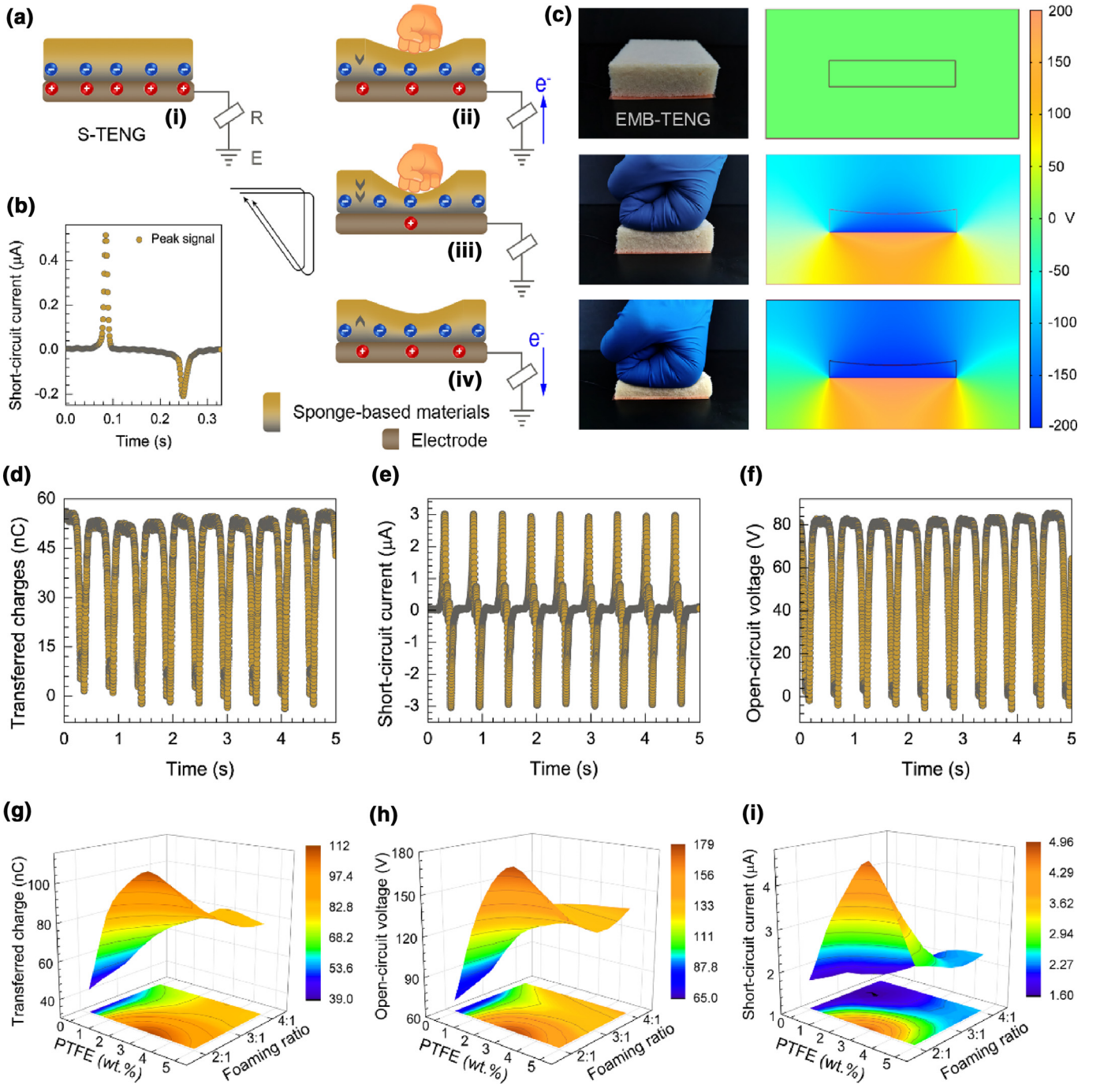

FIGURE 2

Working principle and electrical output performance of elastic-material-based triboelectric nanogenerator (EMB-TENG). (a). Principle of the charge transfer of EMB-TENG under reciprocating compression deformation. (b). Magnified short-circuit current signal of EMB-TENG. (c). The compression process and corresponding potential distribution of EMB-TENGs. (d) Transferred charge amount, (e) short-circuit current, and (f) open-circuit voltage of EMB-TENGs. (g) Transferred charge amount, (h) open-circuit voltage, and (i) short-circuit current of the EMB-TENG under different foaming ratios and PTFE content.

is removing from the triboelectric sponge, the electrons will be repelled back from the Cu electrode to the ground through the external load (iv). By repeatedly pressing and removing force on triboelectric sponge, an alternative current will be generated. Therefore, during the compression and recovery process of fabricated polyurethane triboelectric sponge and Cu film, the current signal can be detected in the circuit (Fig. 2**b**). Because the elastic triboelectric sponge has a three-dimensional porous structure and can generate above 50% elastic deformation, and corresponding simulations of potential distribution in three different states by COMSOL are presented in Fig. 2**c**.

Next, we fixed the EMB-TENG with single-electrode mode on the experimental test platform to test the output-performance of the undoped elastic triboelectric sponge. In order to avoid fatigue

Please cite this article in press as: X. Gao et al., Materials Today (2023), https://doi.org/10.1016/j.mattod.2023.03.010

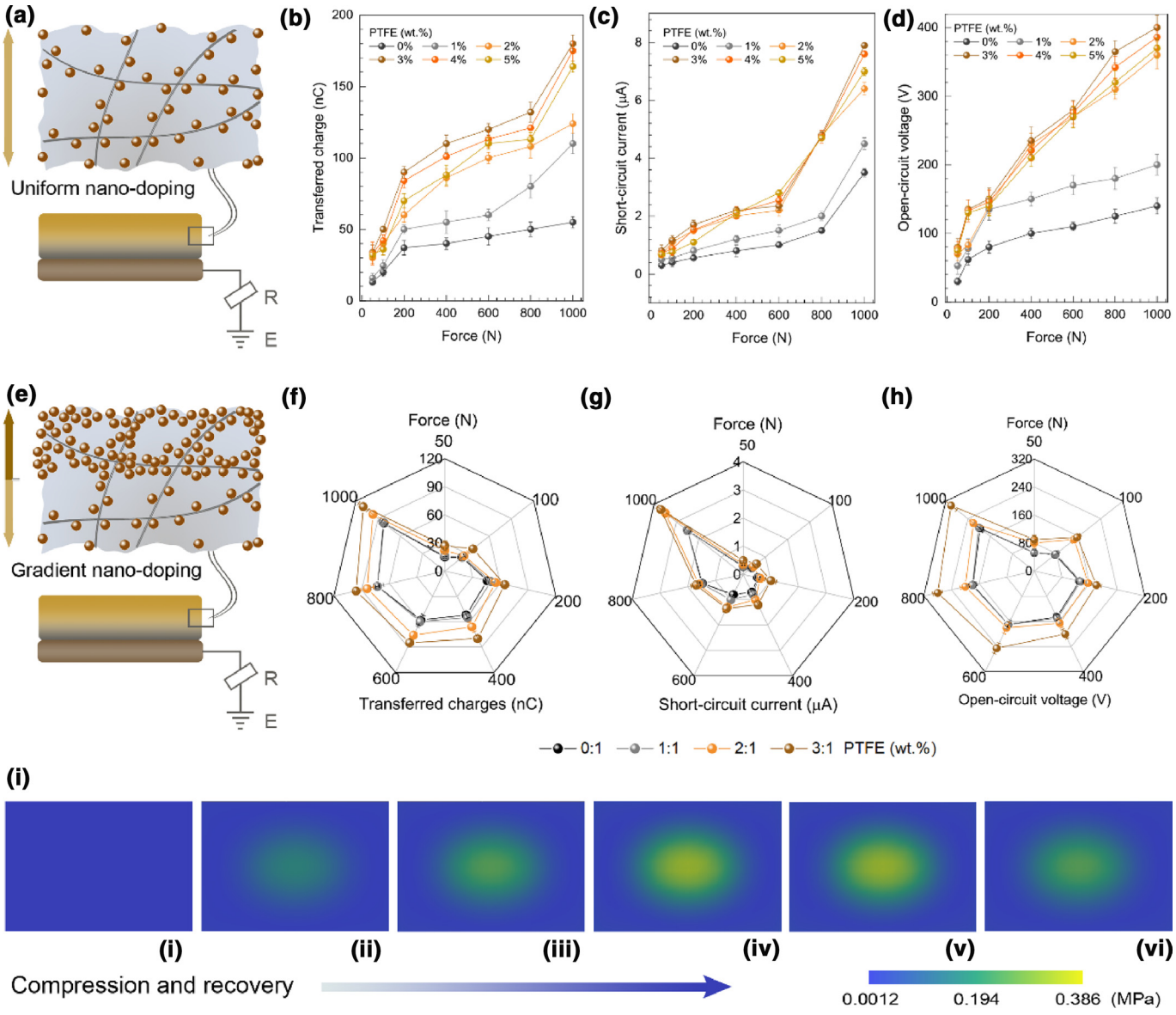

FIGURE 3

Electrical output performance of EMB-TENG with uniform and gradient nano-doped triboelectric materials. (a). Microscopic schematic diagram of uniform nano-doping triboelectric materials. (b). Transferred charge amount, (c) short-circuit current, and (d) open-circuit voltage of uniform nano-doped EMB-TENGs with different PTFE contents and different forces. (e). Microscopic schematic diagram of gradient nano-doped triboelectric materials. (f). Transferred charge amount, (g) short-circuit current, and (h) open-circuit voltage of gradient nano-doped EMB-TENGs with different PTFE contents and different forces. (i) Stress distribution of EMB-TENGs for a process of compression to recovery.

and crack of metal electrode caused by long-term impact as much as possible, we paste the electrode and triboelectric material together. Under the frequency of 2 Hz, the transferred charges, the short-circuit current and the open-circuit voltage reached 50 nC, 3 μA, and 80 V, as shown in Fig. 2**d-f**. In order to improve the output-performance of triboelectric sponge by nano-doping strategy, the foaming ratio and doping content were changed designed to obtain high charge density and sensing sensitivity. The influence of doped triboelectric sponge on the electrical output-performance was discussed, as shown in Fig. 2**g**-i. When the foaming ratio is 2:1 and the doped content of PTFE is 3%, the EMB-TENG has the best electrical output-performance, the transferred charge, the open-circuit voltage and short-circuit current can reach 110 nC, 180 V, and 4.8 μA, respectively. The detailed experimental results are shown in **Fig. S4** in the Supporting Information.

In addition, the electrical output-performances of the uniform nano-doping and gradient nano-doping triboelectric sponge were compared, which aiming to harvest irregular and random mechanical energy to provide a favorable guarantee. First, we tested the transferred charge, short-circuit current and open-circuit voltage of uniform nano-doped triboelectric sponge under different pressures (Fig. 3**a**). The results show that the electrical output-performance firstly increases and then decreases with the increased content of PTFE. Because of the increased content of the PTFE and reaching the critical value, the skeletal matrix

Please cite this article in press as: X. Gao et al., Materials Today (2023), https://doi.org/10.1016/j.mattod.2023.03.010

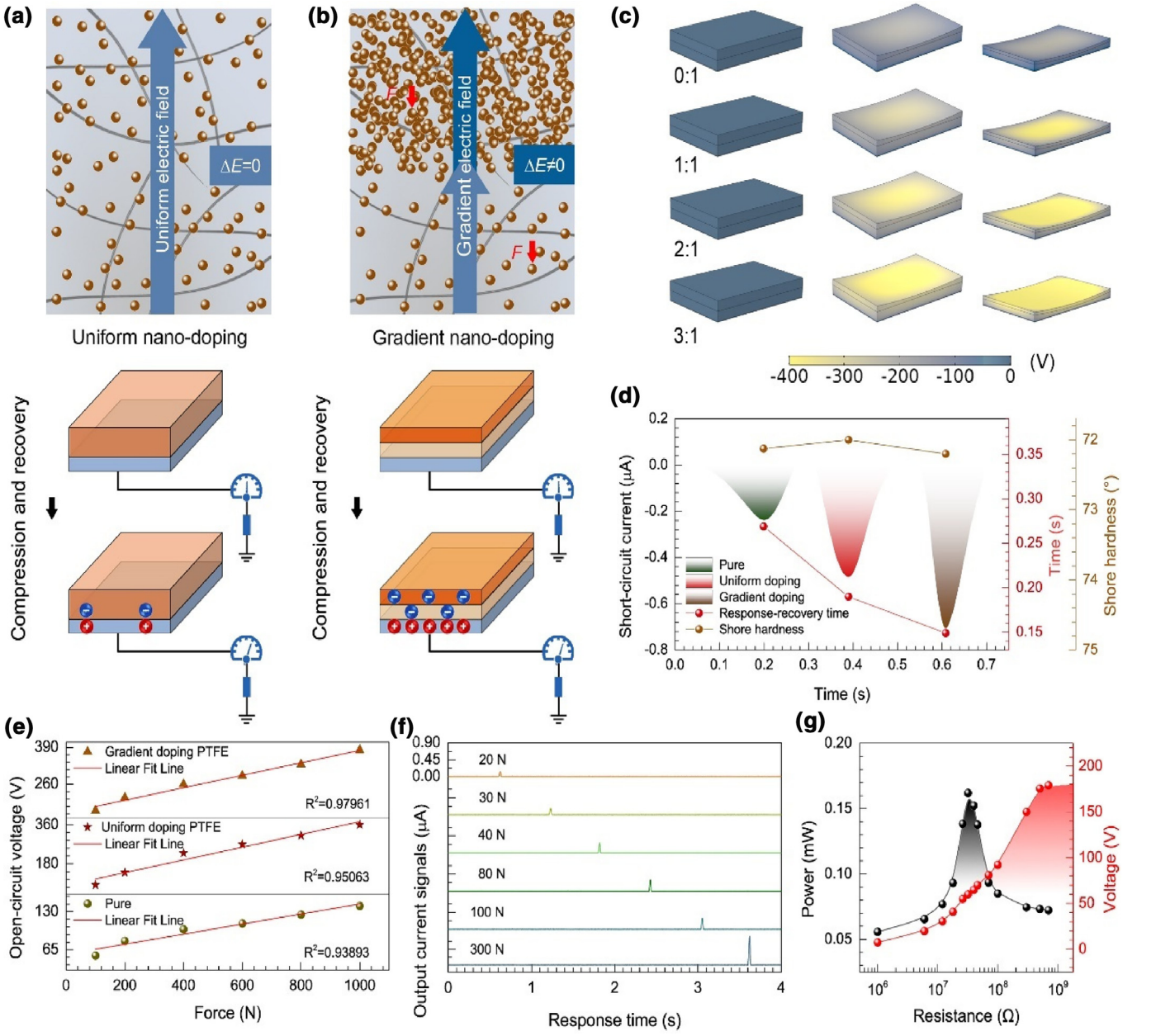

FIGURE 4

Mechanism and sensing performances of EMB-TENG with uniform and gradient nano-doping triboelectric materials. (a). Charge transfer and electric field distribution of uniform nano-doped EMB-TENGs. (b). Charge transfer and gradient electric field distribution of gradient nano-doped EMB-TENGs. (c). Potential simulation of gradient nano-doped EMB-TENGs. (d). Hardness and response-recovery time of EMB-TENGs with different nano-doped triboelectric materials. (e). Output voltages signals of EMB-TENGs with different nano-doped triboelectric materials via different strains induced by different pressures. (f). Output voltage signal of gradient nano-doped EMB-TENGs sensing array under different stress. (g). The output open-circuit voltage and power of EMB-TENG with the different external loading resistance.

structure of the sponge is almost filled, which will lead to the charge cannot be smoothly induced to the surface of the electrode, so that, resulting in the output-performance declined (Fig. 3**b-d**). When the concentration of PTFE added was 3%, the transferred charges, the short-circuit current and the open-circuit voltage reached the maximum values of 180 nC, 7.8 μA, and 400 V, respectively. Finally, the electrical output-performances of the gradient nano-doped sponge were tested at different pressures (Fig. 3**e**). With surprising results, although the output-performance increases with the gradient ratio, and reaches a maximum when the gradient ratio is 3:1. The transferred charge, short-circuit current and open-circuit voltage reached 110 nC, 4 μA, and 300 V compared with the uniform nano-doped sponge with 1% doping, respectively. Due to the gradient ratio is 3:1 and the uniformly doped 1% sponge has the same lower layer concentration, but the amount of trans-

Please cite this article in press as: X. Gao et al., Materials Today (2023), https://doi.org/10.1016/j.mattod.2023.03.010

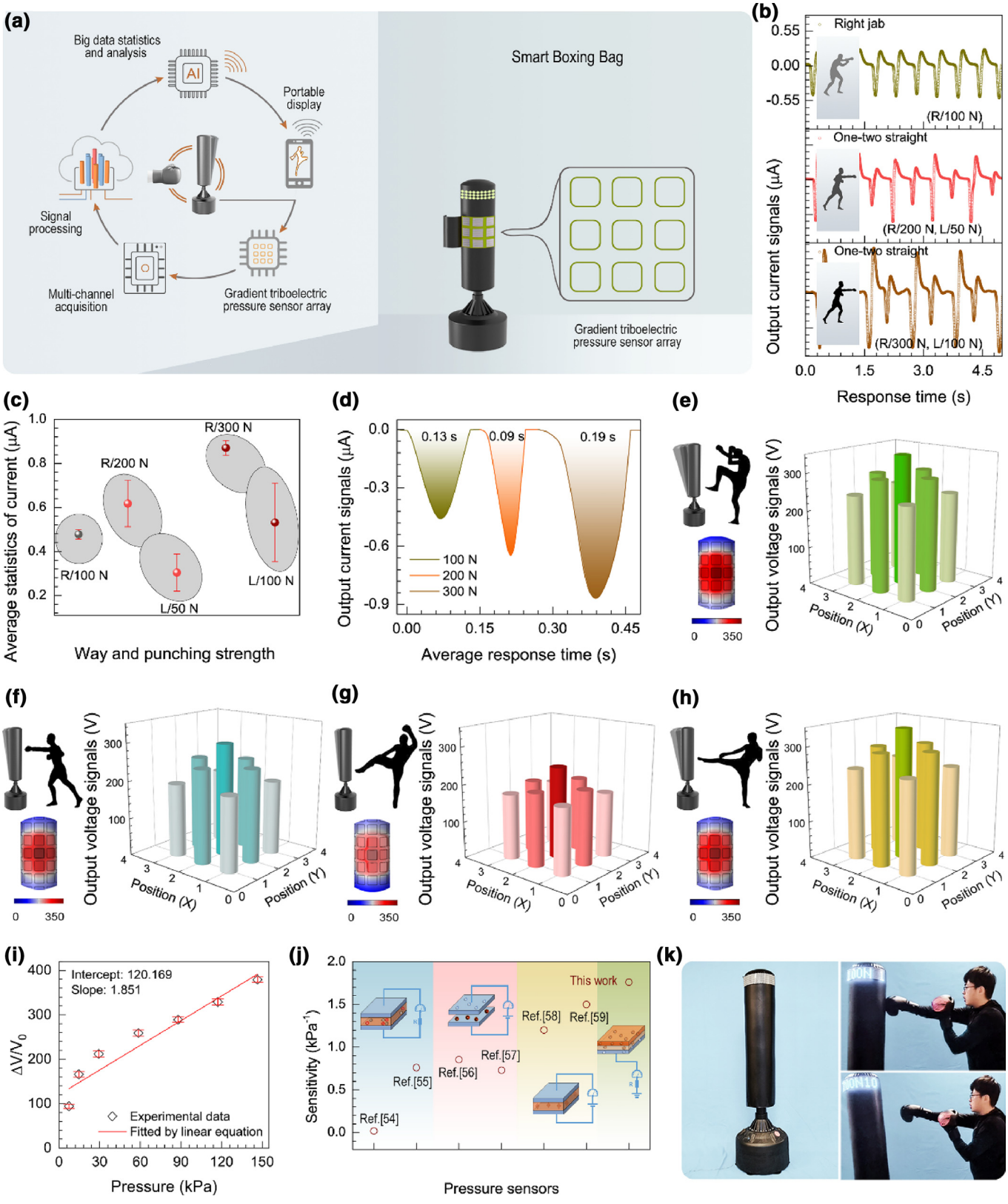

FIGURE 5

Force analysis and real-time counting statistical system of the self-powered smart boxing bag. (a). Schematic diagram of self-powered smart boxing bag (the pressure signals can be converted into a visual statistical result). (b). Output current signals of the self-powered smart boxing bag with different punching postures. (c). Average current signal of the self-powered smart boxing bag with different punching strengths. (d). Response-recovery time of the self-powered smart boxing bag from the forces of 100 N, 200 N, and 300 N. Schematic diagrams of (e). positive kicks, (f). right straight punches, (g). side-kicks and (h). sweeping legs at different positions of the self-powered smart boxing bag, the output voltage of the nine channels and the potential distribution simulation diagram of the corresponding punched and kicked posture by using COMSOL software. (i). Pressure-response curve of EMB-TENG array sensor from the sensitivity of 0 to 150 kPa. (j). Sensitivity comparison of pressure sensors with different working principles. (k). The photos of the self-powered smart boxing bag.

Please cite this article in press as: X. Gao et al., Materials Today (2023), https://doi.org/10.1016/j.mattod.2023.03.010

ferred charge is 1.2 times higher and the output voltage is 1.6 times higher times (Fig. 3**f**-h). Here the gradient ratios (0:1, 1:1, 2:1, and 3:1) in the gradient nano-doped sponge mean that the doping amount of the upper layer opposite to the electrode is 0%, 1%, 2%, 3%, respectively, and the doping concentration of the lower layer where the electrodes meet are all 1%. Both above two different nano-doped triboelectric sponges were tested under the same conditions. The simulation results of the stress distribution during a compression and recovery cycle are shown in Fig. 3**i**. Deformation process and stress simulation of the gradient nano-doped triboelectric sponge materials are shown in **Fig. S5** (Supporting Information).

In order to more clearly explain the reason why the electrical output-performance of gradient doping is higher than that of uniform doping under the same conditions, we have made further analysis from the aspect of interaction electrodynamics. Whether in uniform nano-doping (Fig. 4**a**) or gradient nano-doping (Fig. 4**b**) triboelectric sponges, when the sponge is initially subjected to pressure, the upper layer of the sponge undergoes greater deformation, while the lower layer of the sponge undergoes smaller deformation, so more triboelectric charges are generated internally. According to the charge (Q) calculation formula:

$$Q = \rho_Q S d \tag{1}$$

where ρ_Q is the charge density, S is the contact surface, d is the depth of the compression. There is an electrostatic field around the charges generated by triboelectrification, and the upward direction is defined as the direction of the electric field generated by the positive charges,

$$E = \frac{k_e Q}{r^2} \tag{2}$$

where k_e is the coulomb constant, r is the distance between the charges. The triboelectric charges of gradient doping are higher than that of uniform doping, because of the upper doping concentration of gradient doping is higher than that of uniform doping. Thus, a gradient electric field is generated in a gradient nano-doped sponge, while a uniform electric field is generated in a uniform nano-doped sponge,

$$F = \frac{k_e Q Q_p}{r^2} \tag{3}$$

where Q_p is the amount of charge carried by the other charges. Since the electric field strengths in the two materials are different, the electric field forces on the charges in the two sponges are also different, and the electric field force on the charges in the gradient nano-doped sponge is larger,

$$Q_p = \nabla(\varepsilon_r - 1)\varepsilon_0 E \tag{4}$$

where ∇ is the delta vector operator, ε_r is the permittivity of the triboelectric sponge, ε_0 is the permittivity of vacuum. Combining the equation (1) (2) (3) and (4), we get

$$F_a = \nabla \frac{k_e^2}{r^4}(\varepsilon_r - 1)\varepsilon_0 \rho_{Q_a}^2 S^2 d^2 cos\theta \tag{5}$$

where θ is the angle between horizontal component and the direction of electric force. We think approximately that the charge is subjected to an opposite electric field at the same time. In the same way, we obtain the drag force to the charge.

$$F_r = \nabla \frac{k_e^2}{r^4}(\varepsilon_r - 1)\varepsilon_0 \rho_{Q_r}^2 S^2 d^2 cos\theta \tag{6}$$

According to Newton's second law:

$$m\frac{dv}{dt} = F_a - F_r \tag{7}$$

where m is the mass of charge, d_v and d_t are the differentials of charge velocity and transport time. Combining the equation (5) (6) and (7), we get

$$D_v = \nabla \frac{k_e^2}{mr^4}(\varepsilon_r - 1)\varepsilon_0 S^2 d^2 (\rho_{Q_a} + \rho_{Q_r})(\rho_{Q_a} - \rho_{Q_r}) cos\theta dt \tag{8}$$

therefore, it is found from Equation [57] (8) that when the electric field is larger, the faster the charge moves, the more charge moves per unit time. For uniform nano-doping and gradient nano-doping, there is a larger gradient electric field in the gradient nano-doping sponges, so more charges move to the surface in contact with the electrodes, thereby improving the electrical output-performances. Meanwhile, COMSOL software was used for simulation verification, Fig. 4**c** shows the simulation results of the gradient nano-doped triboelectric sponge. The simulation results of the uniform nano-doped triboelectric sponges are shown in **Fig. S6** (Supporting Information). The results of theoretical derivation and potential simulation are in good agreement with the experimental data, and the gradient nano-doped triboelectric sponge has better electrical output-performances than the uniform nano-doping. The results demonstrate that the proposed a gradient nano-doping strategy can boost the charge density and sensitivity of triboelectric sponge materials via the gradient electrical field caused by the inhomogeneous concentration field of PTFE nanoparticles.

The output current signal, the response-recovery time with the different materials including pure, uniform doping, and gradient doping materials are shown in Fig. 4**d**. When different doping materials, the relationship between the hardness, response and recovery time, the output current signal were studied. The higher output current signal and the shorter response and recovery time were 0.68 μA and 0.15 s at the gradient doping content of 3:1. The output voltages signal of EMB-TENGs with different strains induced by within a range of pressures are also investigated, as shown in Fig. 4**e**. Moreover, the gradient doping material has a high linearity under a large range of pressures which can reach 0.9796, it can be used as an ultrasensitive pressure sensor that is acceptable to the large deformation. The influence of external pressures on EMB-TENG was tested, as shown in Fig. 4**f**. It can be found that EMB-TENG has a good linear response to different pressures, and the value of output current signal increases linearly with the increase of the external pressure. Next, the charging capability of EMB-TENG was tested, the maximum peak output power of 0.15 mW (the volume power density of approximate 732.6 $mW{\cdot}m^{-3}$) can be achieved under an external load resistance of 40 MΩ, as shown in Fig. 4**g**. Therefore, the electrical output performance of EMB-TENG was shown that can high-efficiency convert irregular and random mechanical energy into electricity.

Please cite this article in press as: X. Gao et al., Materials Today (2023), https://doi.org/10.1016/j.mattod.2023.03.010

A self-powered smart boxing bag with the functions of both the force analysis and real-time counting statistical system was further developed benefit from using the gradient nano-doped EMB-TENGs array, that serve as a set of triboelectric pressure sensor to provide real-time statistics assistance and training guidance for both boxing trainees and coaches, as shown in Fig. 5**a**. In order to avoid EMB-TENG array in the boxing bag due to bending deformation, resulting in reduced output performance. A flat groove is cut inside the boxing bag so that the EMB-TENG array is placed parallel. We use a relatively stable current signal which used as a sensing signal to achieve better output-performance, a series of experimental comparison and analysis were carried out on the smart boxing bag. A sensing signal will be generated when a person jabs on the smart boxing bag through the method of multichannel data acquisition. The voltage and current signals of the sensor could be detected at the same time and then the transmitter will send the processed signal to the portable equipment in real-time. Fig. 5**b** shows the current signal generated by a right jab (100 N) and combination blow, including one-two straight (R/200 N, L/50 N) and one-two punch (R/300 N, L/100 N). According to the magnitude of the current signal, the strength and punching method of the person can be monitored in real-time, which can be used for monitoring and analysis of the statistical result, and the trainees' exercise habit data can be gained to assist their training and improve competition tactics. The force and count monitoring system based on the EMB-TENGs array provides a possibility for the manufacture smart equipment for boxing training. The sensing performance of the system with different punching ways and strengths were studied. The high accuracy of EMB-TENG was demonstrated, according to the statistical average current signal value, as shown in Fig. 5**c**. At the same time, the response recovery time of different punching strengths were also characterized under the force of 100 N, 200 N, and 300 N, which the fastest response time by 0.09 s, as shown in Fig. 5**d**. When a person jabs the smart boxing bag in various postures, the different pulse signals will be generated on the triboelectric pressure sensor array, then each sensor connects with the multichannel acquisition. According to the collected voltage signals, the stress characteristics of the high-impact boxing were numerical analyzed.

Fig. 5**e** shows the pressure distributions and simulation diagram of the positive kicking on the smart boxing bag, which the voltage signal range of around 340 V- 240 V from high to low. Therefore, we can know that the attitude is in a forward jabbing from the voltage signals, and the corresponding simulation diagram obtains a sensitive and potential distribution which can also confirm this result. Based on above strategy, the monitoring of different punching postures was also realized including the right straight punch, side kick and sweeping leg that it also has high accuracy and sensitivity, as shown in Fig. 5**f**-h. According to **Fig. S7** in the supporting information, the pressure sensor can maintain stable output performance under high impact. The widespread applicability and stability of the self-powered smart boxing bag were verified in different external forces (Fig. 5**i** and **Fig. S7**). The pressure sensing at large deformation exhibits an almost linear relationship within the upper bound of 150 kPa, and the sensitivity of pressure reaches 1.851 kPa^{-1}. The resolution of the pressure sensor is 10 N. When the pressure is 10 N, the output voltage signal is 10 V. It is also proved that the pressure sensor has high resolution and can accurately respond to the actual pressure. In order to illustrate the sensitivity and linearity of the pressure sensor more accurately, we carried out piecewise fitting of the data, and the fitting results are shown in **Fig. S8** of the supporting information. The compressive rate of the strain can be calculated from formula (9), the maximum strain (ε) of the gradient nano-doped EMB-TENG reach 50%,

$$\varepsilon = \frac{d_0 - d_1}{d_0} \tag{9}$$

where d_0 is the initial thickness of the gradient nano-doped sponge, d_1 is the thickness of the gradient nano-doped sponge under different pressure compression. To verify the sensing performance of EMB-TENG to pressure for application to sensor properties, the elastic triboelectric sensor is compared with previous representative works [58–63] of other working principles (piezoelectric sensor, capacitive sensor, and piezoresistive sensor), showing the superiority of the sensitivity in different pressure ranges, as shown in Fig. 5**j**. Fig. 5**k** exhibits the EMB-TENG used in the scenarios of the smart boxing bag (Supplementary **Video S1**), and a wide applicability of EMB-TENG was displayed. The above have strongly demonstrated the EMB-TENG's ability to sense and its great potential in the area of intelligent sports industry and big data analytics system.

Conclusions

In conclusion, we developed a high-performance elastic-material-based triboelectric nanogenerators (EMB-TENGs) with the large strain for self-powered pressure sensing in boxing equipment and athletic big data analytics. The high-sensitivity triboelectric sponge material was prepared using a novel gradient nano-doping strategy, via gradient electrical field caused by the inhomogeneous concentration field of PTFE nanoparticles. The triboelectric charge density (537 $\mu C \cdot m^{-3}$) and the peak power density (732.6 $mW \cdot m^{-3}$) enhancement of 1.2 times and 1.8 times can be obtained. More importantly, the sensitivity of 1.851 kPa^{-1} which in 50% strain compressive status is successfully realized. Furthermore, a self-powered smart boxing bag with the functions of both the force analysis and real-time counting statistic was further developed benefit from using the gradient nano-doped EMB-TENGs array to provide effective training evaluation and guidance for pugilists and coaches. This research proposes a new way for design and preparation of elastic triboelectric materials at the large strain, and demonstrates applications of highly-sensitive EMB-TENGs in the boxing, which are expected to bring a great opportunity in athletic big data analytics and expanding a new field of sponge-based electronics combining with the self-powered system.

Methods

Preparation of gradient nano-doping triboelectric materials

Polyurethanes are made from polyether polyols and isocyanates foamed in different ratios. The polyether polyols and isocyanates were purchased from Bangpu Chemical Co., LTD. The PTFE was purchased from Huachang plasticizing Co., LTD, PTFE particle size is 200 nm. Copper tape are purchased from Bao Jiaxin flagship store. Based on soft, porous, and elastic deformation charac-

Please cite this article in press as: X. Gao et al., Materials Today (2023), https://doi.org/10.1016/j.mattod.2023.03.010

teristics of polyurethane sponge. Polyurethane elastic sponge was doped with PTFE by a simple room temperature foaming process. According to the calculation, different mass fractions of PTFE nano-powders were added to a certain content of polyether polyols and stirred for 20 minutes to make the PTFE nano-powders evenly dispersed in the polyether polyol solution, and then a certain mass of isocyanate was weighed and added to the mixed solution. In the mixed solution, stir quickly and pour it into the mold quickly to foam for 10 minutes. The solution preparation and foaming process at room temperature are shown in **Fig. S1** in the supporting information. Using the same method, the mixed solution of PTFE powder with different mass fractions was poured into the mold in turn and divided into upper and lower layers for foaming to obtain polyurethane sponges with different concentration gradients of PTFE.

Fabrication of EMB-TENG and pressure sensor array

The EMB-TENG is fabricated with elastic polyurethane sponge (including gradient nano-doped sponge and uniform nano-doped sponge) and copper membrane. The elastic polyurethane sponge is cut into a size of 10.5 cm × 6.5 cm × 3 cm and acts as the triboelectric layer of EMB-TENG. Copper tape is bonded on bottom side of elastic polyurethane sponge as electrode of EMB-TENG. By adjusting the compression and recovery amplitude of EMB-TENG, electrical signals with different compression deformation can be achieved. The EMB-TENG is prepared with gradient nano-doped sponge as the triboelectric layers and the compression deformation is 50%. The EMB-TENG is fabricated with gradient nano-doped triboelectric pressure sensor array. In order to test the sensing property of the elastic polyurethane sponge to pressure, the elastic polyurethane sponge is placed in a linear motor experimental platform, and different pressure is putting on the elastic polyurethane sponge.

Characterization

The surface structure of elastic polyurethane sponge is characterized by Japan SU8020 field emission scanning electron microscope. The three-dimensional morphology of elastic polyurethane sponge is characterized by the American Auto Pore V mercury porosimeter. The hardness of elastic polyurethane sponge is characterized by China Edberg shore hardness tester LX-F. A commercial linear mechanical motor is used to drive the EMB-TENG for measuring its output performance. The transferred charge, open-circuit voltage, and short circuit current were measured using a current preamplifier (Keithley 6514 System Electrometer). The display and storage of data were performed by installing the software LabVIEW on the computer.

CRediT authorship contribution statement

Xiaobo Gao: Data curation, Investigation, Methodology, Writing – review & editing. **Fangjing Xing:** Data curation, Investigation. **Feng Guo:** Supervision. **Jing Wen:** Methodology, Visualization. **Hao Li:** Formal analysis. **Yuhan Yang:** Visualization. **Baodong Chen:** Conceptualization, Resources, Supervision, Writing – review & editing. **Zhong Lin Wang:** Funding acquisition, Writing – review & editing.

Data availability

Data will be made available on request.

Declaration of Competing Interest

The authors declare that they have no known competing financial interests or personal relationships that could have appeared to influence the work reported in this paper.

Acknowledgments

X. G., and F. X. contributed equally to this work. The authors acknowledge the support from National Natural Science Foundation of China (Grant No. 52192610), and National Key R & D Project from Minister of Science and Technology (2021YFA1201601).

Appendix A. Supplementary material

Supplementary data to this article can be found online at https://doi.org/10.1016/j.mattod.2023.03.010.

References

[1] J. Chen et al., Nat. Energy 1 (2016) 16138.
[2] Y. Zou et al., Nano Energy 77 (2020) 105303.
[3] G. Chen et al., Chem. Rev. 120 (2020) 3668–3720.
[4] Z.L. Wang, Nano Energy 58 (2019) 669–672.
[5] B. Chen et al., Mater. Today 50 (2021) 224–238.
[6] D. Liu et al., Nano Energy 73 (2020) 104819.
[7] L. Gao et al., Nano Energy 72 (2020) 104684.
[8] T. Jiang et al., Adv. Energy. Mater. 10 (2020) 2000064.
[9] G. Chen et al., Chem. Rev. 122 (2022) 3259–3291.
[10] A. Libanori et al., Nat. Electron. 5 (2022) 142–156.
[11] J.H. Park et al., Nano Energy 56 (2019) 531–546.
[12] J.H. Han et al., Nano Energy 53 (2018) 198–205.
[13] L. Zhao et al., Nano Energy 28 (2016) 172–178.
[14] J.P. Rojas et al., Nano Energy 31 (2017) 296–301.
[15] Y. Yang et al., Nano Res. 5 (2012) 888–895.
[16] M. Norouzi et al., Thin Solid Films 619 (2016) 41–47.
[17] J. Chang et al., Nano Energy 1 (2012) 356–371.
[18] Z. Pi et al., Nano Energy 7 (2014) 33–41.
[19] H. Yang et al., Nano Energy 56 (2019) 300–306.
[20] Y. Guo et al., Nano Energy 60 (2019) 641–648.
[21] J. Han et al., Adv. Funct. Mater. (2021) 2108580.
[22] X. Fu et al., ACS Energy Lett. (2021) 2343–2350.
[23] C. Zhang et al., ACS Energy Lett. (2021) 1490–1499.
[24] Y. Wang et al., Nano Energy 82 (2021) 105740.
[25] X. Gao et al., Mater. Today Energy 22 (2021) 100867.
[26] J. Zhang et al., ACS Appl. Mater. Interfaces 13 (2021) 55136–55144.
[27] Y. Wang et al., ACS Nano 15 (2021) 15700–15709.
[28] H. Pang et al., Adv. Funct. Mater. (2021) 2106398.
[29] Z. Ren et al., Adv. Energy Mater. (2021) 2101116.
[30] T.X. Xiao et al., Adv. Funct. Mater. 28 (2018) 1802634.
[31] C. Zhang et al., Joule 5 (2021) 1–11.
[32] B.D. Chen et al., Mater. Today 21 (2018) 88–97.
[33] Y. Yang et al., Adv. Funct. Mater. (2022) 2200521.
[34] C. Wu et al., IEEE Sens. J. 20 (2020) 13999–14006.
[35] G. Khandelwal et al., Appl. Energy 219 (2018) 338–349.
[36] F.R. Fan et al., J. Mater. Chem. A 2 (2014) 13219–13225.
[37] F.R. Fan et al., Nano Energy 1 (2012) 328–334.
[38] Y. Yang et al., ACS Nano 7 (2013) 9461–9468.
[39] Z.L. Wang, ACS Nano 7 (2013) 9533–9557.
[40] Z.L. Wang, Faraday Discuss. 176 (2014) 447–458.
[41] Z.L. Wang, Mater. Today 20 (2017) 74–82.
[42] Z. Xie et al., Extreme Mech. Lett. 37 (2020) 100713.
[43] Z. Wu et al., Sensors - Basel 20 (2020) 2925.
[44] Z. Wang et al., ACS Nano 14 (2020) 5981–5987.
[45] J. Chen et al., Adv. Mater. Technol. 4 (2019) 1900337.
[46] Y. Hao et al., ACS Nano 16 (2022) 1271–1279.
[47] S. Wang et al., J. Mater. Chem. A 4 (2016) 3728–3734.

Please cite this article in press as: X. Gao et al., Materials Today (2023), https://doi.org/10.1016/j.mattod.2023.03.010

[48] W. Tang et al., Adv. Funct. Mater. 25 (2015) 3718–3725.
[49] J. Wang et al., Nat. Commun. 8 (2017) 88.
[50] L. Xu et al., Nano Energy 49 (2018) 625–633.
[51] L. Zhang et al., Nano Energy 16 (2015) 516–523.
[52] T.-C. Hou et al., Nano Energy 2 (2013) 856–862.
[53] M.-H. Yeh et al., Adv. Funct. Mater. 26 (2016) 1054–1062.
[54] Q. Zheng et al., Adv. Funct. Mater. 28 (2018) 1706365.
[55] X. Cui et al., Nano Energy 78 (2020) 105381.
[56] H.-Y. Mi et al., Nano Energy 48 (2018) 327–336.
[57] Q. Sun et al., Nat. Mater. 18 (2019) 936–941.
[58] S. Kim et al., ACS Appl. Mater. Interfaces 11 (2019) 16006–16017.
[59] D.Y. Park et al., Adv. Mater. 29 (2017) 1702308.
[60] R.Y. Tay et al., Adv. Funct. Mater. 30 (2020) 1909604.
[61] A. Chhetry et al., Adv. Funct. Mater. 30 (2020) 1910020.
[62] J. Shi et al., Small 14 (2018) 1800819.
[63] L. Gao et al., ACS Appl. Mater. Interfaces 11 (2019) 25034–25042.

Please cite this article in press as: X. Gao et al., Materials Today (2023), https://doi.org/10.1016/j.mattod.2023.03.010